Antiviral Research 100 (2013) 673–687

Contents lists available at ScienceDirect

Antiviral Research

journal homepage: www.elsevier.com/locate/antiviral

Proteomic analysis at the subcellular level for host targets against influenza A virus (H1N1)

Haibao Zhao [a,1], Jing Yang [a,1], Kang Li [a,1], Xiaoran Ding [a], Ruxian Lin [a], Yongjie Ma [a], Juan Liu [a], Zhiyin Zhong [a], Xiaohong Qian [a], Xiaochen Bo [a], Zhe Zhou [a,*], Shengqi Wang [a,b,*]

[a] Beijing Institute of Radiation Medicine, Beijing 100850, PR China
[b] Traditional Chinese Medicine of Henan University, Zhengzhou 450003, PR China

ARTICLE INFO

Article history:
Received 16 March 2011
Revised 10 October 2013
Accepted 14 October 2013
Available online 22 October 2013

Keywords:
Influenza virus
Proteomic analysis
Host target
H1N1

ABSTRACT

Influenza viruses (IVs) trigger a series of intracellular signaling events and induce complex cellular responses from the infected host cell. Accumulating evidence suggests that host cell proteins play an essential role in viral propagation and represent novel antiviral therapeutic targets. Subcellular proteomic technology provides a method for understanding regional differences at the protein level. The present study, which utilized subcellular proteomic technology, aimed to identify host cell proteins involved in influenza virus (HIN1) infection. Two-dimensional gel electrophoresis (2-DE) combined with mass spectrum (MS) was performed on protein extracts from the nuclei, cytoplasm, and mitochondria of infected and control human lung epithelial cells (A549). In total, 112 differentially expressed protein molecules were identified; 80 protein spots were successfully validated using MS. The differential expression of ISG15, MIF, PDCD5, and UCHL1 was confirmed by western blot. Furthermore, antisense oligodeoxyribonucleotide (ODN) targeting ISG15, MIF, PDCD5, and UCHL1 significantly mitigated HIN1 propagation, cytopathic effects, vRNA by RT-qPCR, and rescued cell viability in A549 cells. Taken together, the differentially expressed proteins identified in this study might provide novel targets for anti-influenza drug development.

1. Introduction

Influenza viruses are among the most common causes of human respiratory infections and cause high morbidity and mortality. Influenza viruses belong to the *Orthomyxovirus* genus and Orthomyxoviridae family. Influenza viruses are divided into three different types, that is, A-, B-, and C-type viruses, based on their nucleocapsid and M protein antigens. Among these, influenza A viruses exhibit the broadest host spectrum (birds, humans, and other mammals) and have the potential to evolve into highly pathogenic strains (Chen and Deng, 2009; Li and Freedman, 2009). In addition to annual winter outbreaks, pandemic influenza A viruses occasionally emerge during other seasons (Li and Freedman, 2009). Over the past 120 years, influenza A pandemics occurred in 1889, 1918, 1957, and 1968, and the pandemic of 1957 killed up to 50 million people worldwide (Morens and Fauci, 2007; Simonsen, 1999). Influenza viruses are impossible to eradicate as there is a large reservoir of influenza virus subtypes in wild aquatic birds and other animals that can contribute genes to new pathogenic virus variants (Shortridge et al., 2000). In April 2009, a new H1N1 influenza A virus pandemic occurred, which was first identified in Mexico and then spread rapidly to other regions around the world (Cohen, 2009). The continuous emergence of new virus variants poses a major problem for the design and development of antiviral therapies (Bridges et al., 2003; Gubareva et al., 2002).

Influenza viruses trigger a series of intracellular signaling events and induce complex cellular responses. Many proteins have been demonstrated to be involved in influenza virus-induced responses among mammals. Several of these proteins were found to play an essential role in viral attenuation (Ehrhardt and Ludwig, 2009; Ehrhardt et al., 2007; Mazur et al., 2007; Turpin et al., 2005; Wurzer et al., 2003). For example, caspase 3 is crucial for efficient influenza viral propagation since influenza virus propagation is compromised in the presence of a caspase 3 inhibitor and in cells where caspase 3 is partially knocked down by small interfering RNAs (siRNAs) (Wurzer et al., 2003). Turpin et al. suggested that p53 levels and activities are upregulated during influenza infection. Specifically, they showed that p53 is required for influenza-induced cell death and that the inhibition of p53 leads to increased viral titers (Turpin et al., 2005). Therefore, better understanding of cellular cofactors, which are essential for virus propagation, might lead to the development of new antiviral therapies.

* Corresponding authors. Address: Laboratory of Biotechnology, Beijing Institute of Radiation Medicine, No. 27, Tai Ping Road, Beijing 100850, PR China. Tel./fax: +86 10 66932211.
E-mail addresses: zhouzhe@bmi.ac.cn (Z. Zhou), sqwang@bmi.ac.cn (S. Wang).
[1] These authors contributed equally to this work.

0166-3542/$ - see front matter © 2013 Elsevier B.V. All rights reserved.
http://dx.doi.org/10.1016/j.antiviral.2013.10.005

The proteomic approach appears to be an ideal method for identifying both viral proteins and cell signaling molecules in influenza virus-infected host cells. However, due to the complexity of eukaryotic cells, it is difficult to identify differential proteins from whole cell lysates by two-dimensional electrophoresis (2-DE). One approach to solving this is to study subcellular regions and compartments (Baas et al., 2006; Liu et al., 2008; Morrissey and Downard, 2006; Shaw et al., 2008). Subcellular proteomics is a flexible approach that reduces sample complexity and can be efficiently combined with mass spectrometry (MS) analysis (Kislinger et al., 2006).

A recent study utilizing the subcellular proteomics method investigated the subcellular location of several key proteins involved in cell death as well as in antiviral and stress responses, which are regulated during infection with influenza A virus, on human primary macrophages (Ohman et al., 2009). However, since the epithelial cells of the upper respiratory tract are the primary target of influenza viruses, it is important to understand the molecular mechanism underlying influenza virus-induced injuries in airway epithelial cells. The present study was designed to study the effects of influenza virus (H1N1) infection on the nuclear, mitochondrial, and cytosolic protein profiles of human lung epithelial cells by utilizing a subcellular comparative proteomic approach. Our findings indicate that the translocation of macrophage inhibitory factor (MIF), ubiquitin carboxyl-terminal esterase L1 (UCHL1), and programmed cell death protein 5 (PDCD5) is a crucial event for efficient propagation of the influenza virus.

2. Materials and methods

2.1. Cells, virus, and in vitro antiviral assays

A549 cells were purchased from the American Type Cell Collection (ATCC, Manassas, USA) and were cultured in 1640 medium supplemented with 10% fetal bovine serum (FBS), 100 U/mL penicillin, and 100 μg/mL streptomycin under standard conditions (37 °C in a humidified atmosphere containing 5% CO_2). Influenza A/jingfang/1/86 (H1N1) virus was grown in the allantoic cavity of 10-d-old embryonated chicken eggs (Specific Pathogen Free, SCXK-BJ-2009-0003, Merial Vital Laboratory Animal Technology, Beijing, China) for 48 h at 35 °C. The allantoic fluid was cleared by centrifugation at 6000×*g* for 15 min and stored at −80 °C until use. The experiments were reviewed and were approved by the Animal Ethics Committee of the Beijing Institute of Radiation Medicine in accordance with the regulations of Beijing Administration Office of Laboratory Animal.

The antiviral efficiency of antisense oligodeoxynucleotide (ODN) in cultured A549 cells was determined by the inhibition of virus-induced cytopathic effects (CPEs). In order to avoid the quick occurrence of cytopathic effect but showing a high infectivity, the H1N1 virus was inoculated at a multiplicity of infection (MOI) of 1.38 (75% tissue culture infective dose) in 1640 medium supplemented with 1 μg/ml trypsin in the absence of FBS (He et al., 2010). After inoculation, the cells were washed twice in phosphate–buffered saline (PBS) to remove unabsorbed viruses, and fresh conditional media were added to each well with varying concentrations of ODN. The cells were then incubated for another 48 h. Cell viability was tested using the MTS assay (CellTiter-96®AQueous One Solution Reagent assay systems, Promega). Each experiment was performed in triplicate and repeated three times.

2.2. Organelle isolation

Cell and organelle preparation was performed as previously described (Kislinger et al., 2006). The cells were quickly washed three times in ice-cold PBS and homogenized in ice-cold lysis buffer (250 mM sucrose, 50 mM Tris–HCl [pH 7.4], 5 mM $MgCl_2$, 1 mM dithiothreitol [DTT], and 1 mM phenylmethylsulfonyl fluoride [PMSF]) by using a tight-fitting Teflon pestle (all subsequent steps were performed at 4 °C or on ice). The lysate was centrifuged using a benchtop centrifuge at 800×*g* for 15 min with the supernatant containing the cytosolic, mitochondrial, and microsomal fractions. The nuclear pellet was re-homogenized in lysis buffer, re-centrifuged, and solubilized in 6 mL of cushion buffer (2 M sucrose, 50 mM Tris–HCl [pH 7.4], 5 mM $MgCl_2$, 1 mM DTT, and 1 mM PMSF). After overlaying 2 mL of cushion buffer, the nuclear pellet was reobtained by ultracentrifugation at 80,000×*g* for 1 h (Beckman MLA-80 rotor). The mitochondria were isolated from the crude cytoplasm by centrifugation at 6000×*g* for 15 min, and the resulting pellet was washed twice with lysis buffer. The supernatant was centrifuged at 100,000×*g* for 1 h (Beckman MLA-80); the supernatant served as a cytosolic fraction and was stored at −80 °C.

2.3. Protein extraction

Nuclear proteins were extracted by resuspending the nuclear pellet in lysis buffer II (8 M urea, 2 M thiourea, 4% CHAPS, 65 mM DTT, 1 mM PMSF, 0.5% immobilized pH gradient [IPG] buffer), followed by 30 min incubation with gentle shaking. The debris was removed by centrifugation at 13,000×*g* for 30 min. The supernatant was saved and stored at −80 °C. Mitochondrial proteins were isolated by incubating the isolated mitochondria in the hypotonic lysis buffer (10 mM HEPES [pH 7.9], 1 mM DTT, and 1 mM PMSF) for 30 min on ice. The suspension was briefly sonicated, and the debris was removed by centrifugation at 13,000×*g* for 30 min. The supernatant was stored at −80 °C.

2.4. Two-dimensional electrophoresis (2-DE) and imaging analyses

2-DE and imaging analyses were performed as previously reported (Lin et al., 2009). Briefly, 2 mg (for a pH 4–7 IPG strip) of protein was diluted with 450 μL of rehydration solution containing 8 M urea, 0.5% CHAPS, 0.5% IPG buffer (pH 3–10 or pH 4–7), and 0.2% DTT and was then loaded onto 24 cm IPG strips (GE Healthcare) with a pH 4–7. The total Vh was 80,000–100,000. First-dimensional isoelectric focusing (IEF) was carried out according to the manufacturer's protocols. After the IEF separation, the gel strips were immediately equilibrated with buffer I (6 M urea, 30% glycerol, 2% sodium dodecyl sulfate [SDS], and 1% DTT) and then buffer II (DTT replaced with 2.5% iodoacetamide) for 15 min each. Second-dimension separation was performed on 12.5% polyacrylamide gels at 20 mA/gel and then with a 40 mA/gel constant current until the bromophenol blue front reached the bottom of the gel. The gels were stained with Coomassie Brilliant Blue G-250 or silver staining and scanned with an ImageScanner (GE Healthcare) in transmission mode. Spot detection and matching were performed using ImageMaster 2D Elite 4.01 (GE Healthcare).

2.5. In-gel digestion and matrix-assisted laser desorption/ionization-time-of-flight mass spectroscopy (MALDI-TOF MS)

In-gel digestion of proteins from 2-DE gels was performed as described earlier (Steiner et al., 2000). Spots were excised and destained with 25 mM ammonium bicarbonate/50% acetonitrile and dried in a vacuum concentrator (Savant, Holbook, NY). The dried gel pieces were rehydrated with 5 μL of 20 mg/L trypsin and digested at 37 °C for 18–20 h. Tryptic peptides were first extracted using 5% trifluoroacetic acid (TFA) at 40 °C for 1 h and then 2.5% TFA/50% acetonitrile at 30 °C for 1 h. The extracted solutions were mixed in an Eppendorf tube and dried in a vacuum concentrator.

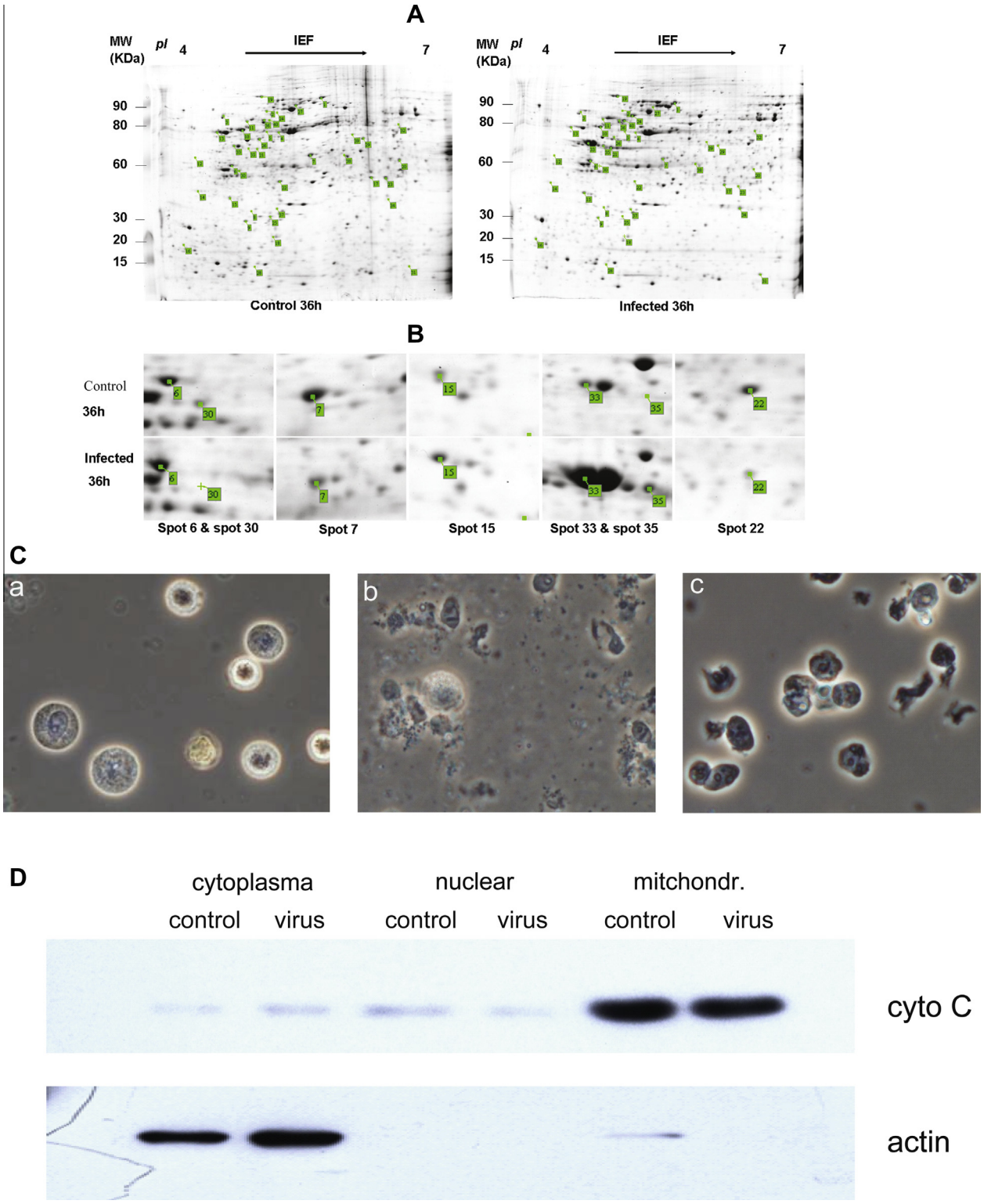

Fig. 1. Two-dimensional gel electrophoresis (2-DE) of A549 cell nuclear protein extracts from control and influenza A/jingfang/1/86 (H1N1) virus infected cells. Representative 2-DE images of nuclear proteins from one pair of controls versus the 36 h group after infection (MOI = 1.38). (A) The proteins from control and infected A549 cells were separated on IPG strips followed by SDS–PAGE on 12.5% gel. The gels were stained with Coomassie Brilliant Blue G-250. Differential expression of proteins was marked by a label with a number. (B) Enlarged 2-DE images of differentially expressed spots. (C) Purity of subcellular fractions observed by contrast-phase microscopy. (a) Intact isolated A549 cells; (b) cytosolic and nuclear lysates; (c) nuclear fraction purified from (b). (D) Western blot detection of actin and cytochrome *c* in the subcellular fractions. (E) The images of A549 cells after inoculation of influenza A H1N1 virus, as observed by contrast-phase microscopy. (F) Apoptotic analysis using influenza A H1N1 virus-infected A549 cells as detected by Hoechst 33,258 staining. (G) NP protein expression in the cytosolic and nuclear fractions of virus-infected A549 cells at different time points as detected by western blotting. Actin was used as the reference protein for the cytoplasm protein and Ref-1 was used as the reference protein for the nuclear protein. Data shown are representative of three independent experiments.

The peptide mixture was solubilized with 0.5% TFA for MS analysis. The MS was performed on a Reflex MALDI-TOF MS (Bruker Daltonics, Bremen, Germany) with saturated α-cyano-4-hydroxy-trans-cinnamic (CHCA) solution in 0.1% TFA/50% acetonitrile as the matrix. Mass spectra were externally calibrated with auto-digest peaks of trypsin (MH+: 906.505, 1020.504, 1153.574, 2163.057, and 2273.160 Da).

2.6. Database searching

Database searches were performed using the MASCOT program (http://www.matrixscience.com). The search parameters utilized are described in Lim et al. (2003): (1) peptide mass tolerance of 0.1 Da, (2) minimum number of peptide matches of two, (3) minimum sequence coverage of 10%, and (4) cysteine modification by iodoacetamide and methionine oxidation.

2.7. Western blot analysis

Thirty micrograms of protein from A549 cells was separated using a 12% SDS–PAGE gel. The proteins were then transferred onto PVDF membranes. The membranes were blocked with 5% (w/v) non-fat dry milk in Tris–buffered saline (TBS)/0.1% Tween-20 at room temperature for 1 h and then incubated with the specific primary antibody (diluted 1:1000 in 2.5% [w/v] non-fat dry milk in TBS/0.1% [v/v] Tween-20) overnight at 4 °C. After three washes with TBS/0.1% (v/v) Tween-20, the membranes were incubated with the appropriate horseradish peroxidase-conjugated secondary antibody for 1 h at room temperature. The blots were developed using the enhanced chemiluminescence (ECL) detection system (GE Healthcare) according to the manufacturer's protocols. Quantitative data normalized to reference gene were obtained using a densitometer and analyzed with the Quantity One 4.4.0 software (BIO-RAD). Actin was used as the reference gene for the cytoplasm protein and the Ref-1 was used as the reference gene for nuclear proteins.

2.8. Effect of antisense oligodeoxynucleotides (ODNs) on influenza virus-induced CPE on A549 cells

ODNs targeting ISG15, MIF, PDCD5, and UCHL1 were designed using computer-assisted software (sense sequences used as controls). The A549 cells were incubated with ODNs or controls for 1 h and then inoculated with the virus. After 2 d, the cells were harvested for the indicated analyses. CPE was measured by cell viability with the CellTiter-96®AQueous One Solution Reagent assay system according to the manufacturer's instructions. Total proteins were isolated and subjected to western blotting for the detection of proteins expression by using anti-PDCD5, MIF, ISG15 or anti-UCHL1 antibodies.

2.9. Viral RNA detection in the culture medium by quantitative real-time polymerase chain reaction (qRT-PCR)

The number of virions released in the culture medium was determined using absolute quantification by qRT-PCR. Total RNA was extracted from culture medium by using an RNeasy RNA extraction kit (Qiagen). The qRT-PCR method for influenza A (H1N1) detection recommended by the World Health Organization (http://www.who.int/csr/resources/publications/swineflu/CDCrealtimeRTPCRprotocol_20090428.pdf) was used. The qRT-PCR primers were as follows: Forward, GACCRATCCTGTCACCTCTGAC; Reverse, GGGCATTYTGGACAAAKCGTCTACG. The probe sequence

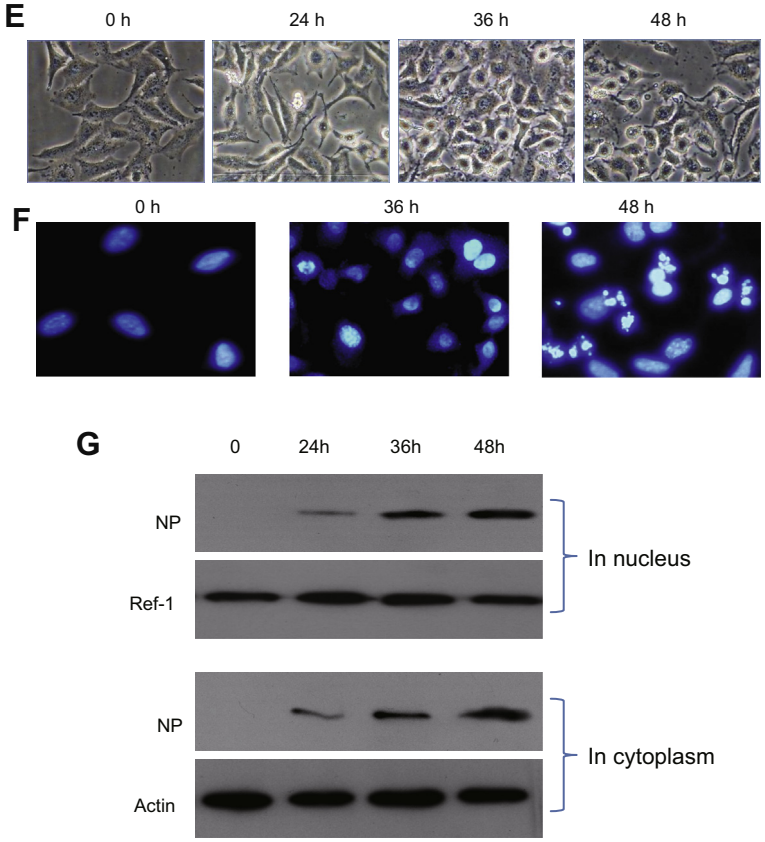

Fig. 1 (*continued*)

Table 1
Identified proteins that changed significantly in A549 cell nuclei after infection.

Spot no.	Protein	Accession no.	Up/down regulated (>2-fold)	Sequence coverage (%)	Score	Mass	*pI*	*P* value	Function	Process
1	Far upstream element-binding protein variant	IPI00788671	Up	11	106	67,431	7.18	1.70E-06	Single-stranded DNA binding, transcription factor activity	Phosphate transport, regulation of transcription, DNA-dependent, transcription, transcription from RNA polymerase II promoter
2	Stress-induced-phosphoprotein 1 (STIP1)	gi|54696884	Down	34	331	62,599	6.4	1.00E-28	Binding	Response to stress
3	Heat shock 70 kDa protein 9B precursor	gi|24234688		15	232	73,635	5.87	8.20E-19	ATP binding, nucleotide binding, unfolded protein binding	Anti-apoptosis, protein export from nucleus, protein folding
4	2-Phosphopyruvate-hydratase alpha-enolase, carbonate dehydratase	gi|693933	Down	19	214	47,079	7.01	5.20E-17	Lyase activity, magnesium ion binding, phosphopyruvate hydratase activity, protein binding, serine-type endopeptidase activity, transcription corepressor activity, transcription factor activity	Glycolysis, negative regulation of cell growth, negative regulation of transcription from RNA polymerase II promoter, transcription
5	ENO1 protein	gi|29792061	Down	26	428	47,139	7.01	2.10E-38	Lyase activity, magnesium ion binding, phosphopyruvate hydratase activity, protein binding, serine-type endopeptidase activity, transcription corepressor activity, transcription factor activity	Glycolysis, negative regulation of cell growth, negative regulation of transcription from RNA polymerase II promoter, transcription
6	Tubulin, beta polypeptide	gi|57209813	Up	27	353	47,736	4.7	6.50E-31	GTP binding, GTPase activity, MHC class I protein binding, nucleotide binding, structural constituent of cytoskeleton	Cell motion, microtubule-based movement, natural killer cell mediated cytotoxicity, protein polymerization, spindle assembly
8	ECHS1 enoyl-CoA hydratase, mitochondrial precursor	IPI00024993	Up	12	103	31,367	8.34	3.30E-06	Enoyl-CoA hydratase activity, lyase activity, protein binding	Fatty acid beta-oxidation, fatty acid metabolic process, generation of precursor metabolites and energy, lipid metabolic process
9	Heat shock protein 27	gi|662841	Down	39	384	22,313	7.83	5.20E-34	Identical protein binding	Anti-apoptosis, cell motion, regulation of translational initiation, response to heat, response to unfolded protein
10	KRT8 protein	gi|33875698	Down	43	550	55,787	5.62	2.60E-28	Protein binding, structural molecule activity, cytoskeleton organization and biogenesis	Cytoskeleton organization and biogenesis, response to other organism
11	Protein disulfide-isomerase (EC 5.3.4.1) ER60 precursor	gi|7437388	Up	24	177	56,761	5.98	2.60E-13	Cysteine-type endopeptidase activity, isomerase activity, phospholipase C activity, protein binding, protein disulfide isomerase activity,	Cell redox homeostasis, positive regulation of apoptosis, protein import into nucleus, protein retention in ER lumen, signal transduction
12	Isoform 2 of nucleophosmin (NPM1)	IPI00220740	Down	36	213	29,446	4.47	3.30E-17	NF-kappaB binding, RNA binding, Tat protein binding, nucleic acid binding IEA, protein heterodimerization activity, protein homodimerization activity, transcription coactivator activity, unfolded protein binding	Activation of NF-kappaB transcription factor, anti-apoptosis, cell aging, centrosome cycle, intracellular protein transport, negative regulation of cell proliferation, nucleocytoplasmic transport, response to stress, ribosome assembly, signal transduction
13	PREDICTED: similar to heat shock cognate 71 kDa protein	gi|57085907	Down	16	257	70,854	5.37	2.60E-21	ATPase activity, coupled, protein folding; response to unfolded protein	Unknown
14	PREDICTED: similar to tropomyosin 3, gamma isoform 27	gi|55593362	Down	50	407	29,015	4.75	2.60E-36	Unknown	Unknown
15	Annexin I	gi|442631	Up	49	622	35,018	7.77	8.20E-58	Calcium ion binding, calcium-dependent phospholipid binding, phospholipase A2 inhibitor activity, protein binding, bridging, receptor binding, structural molecule activity	Anti-apoptosis, arachidonic acid secretion, cell cycle, cell motion, cell surface receptor linked signal transduction, inflammatory response, keratinocyte differentiation, lipid metabolic process, peptide cross-linking, regulation of cell proliferation
16	50 kDa Protein, PREDICTED: similar to Huntingtin-interacting protein 1-related protein	IPI00789998	Up	16	69	49,532	11.18	0.0082	Actin binding, biological_process actin binding, phospholipid binding	Biological_process

(*continued on next page*)

Table 1 (*continued*)

Spot no.	Protein	Accession no.	Up/down regulated (>2-fold)	Sequence coverage (%)	Score	Mass	*pI*	*P* value	Function	Process
17	Heat shock 70 kDa protein 8 isoform 2 (HSPA8)	gi|24234686	Down	30	589	53,484	5.62	1.60E-54	ATP binding, ATPase activity, coupled, nucleotide binding, protein binding.	Protein folding, response to unfolded protein.
18	Splicing factor, arginine/serine-rich 3	gi|30582873	Down	21	79	19,318	11.64	0.0016	Protein binding, RNA binding, nucleotide binding.	RNA splicing, nuclear mRNA splicing, via spliceosome
19	Chain B, crystal structure of the moesin ferm domainTAIL DOMAIN complex	gi|8569618	Up	24	134	34,440	8.92	5.20E-09	Unknown	Unknown
20	Human muscle fructose 1,6-bisphosphate aldolase complexed with fructose 1,6-bisphosphate	gi|4930291	Down	22	152	39,264	8.39	8.20E-11	Unknown	Unknown
22	Annexin A1	IPI00218918	Down	53	746	38,559	6.64	1.70E-70	Calcium ion binding, protein binding, bridging, receptor binding, structural molecule activity,	Anti-apoptosis, arachidonic acid secretion, cell cycle, cell motion, cell surface receptor linked signal transduction, inflammatory response, keratinocyte differentiation, lipid metabolic process, peptide cross-linking, regulation of cell proliferation
25	Nucleophosmin 1 isoform 3	IPI00658013	Down	37	98	28,383	4.56	1.00E-05	NF-kappaB binding, RNA binding, Tat protein binding, nucleic acid binding, protein heterodimerization activity, protein homodimerization activity, transcription coactivator activity, unfolded protein binding	Activation of NF-kappaB transcription factor, anti-apoptosis, cell aging, centrosome cycle, intracellular protein transport, negative regulation of cell proliferation, nucleocytoplasmic transport, response to stress, ribosome assembly, signal transduction
26	Heat shock 70 kDa protein 1A	IPI00514377	Down	29	359	69,995	5.48	8.40E-32		Protein metabolism and modification, immunity and defense
27	Stress-70 protein, mitochondrial precursor	IPI00007765	Down	37	515	73,635	5.87	2.10E-47	ATP binding, nucleotide binding, unfolded protein binding,	Anti-apoptosis, protein export from nucleus, protein folding.
29	SFPQ isoform long of splicing factor, proline- and glutamine-rich	IPI00010740	Down	24	220	76,102	9.45	6.70E-18	DNA binding, RNA binding, nucleotide binding, protein binding	DNA recombination, DNA repair, RNA splicing, mRNA processing, regulation of transcription, DNA-dependent, transcription
30	Isoform 4 of heterogeneous nuclear ribonucleoproteins C1/C2 (HNRNPC)	IPI00759596	Down	31	136	27,804	4.55	1.70E-09	RNA binding, identical protein binding, nucleotide binding	RNA splicing, PubMed 3110598 TAS PubMed, nuclear mRNA splicing, via spliceosome
32	PA2G4 41 kDa protein	IPI00794875	Up	47	273	41,237	6.82	3.30E-23	RNA binding, cobalt ion binding, hydrolase activity, metalloexopeptidase activity, methionyl aminopeptidase activity, protein binding, transcription factor activity	Cell cycle arrest, cell proliferation, negative regulation of transcription, DNA-dependent, proteolysis, rRNA processing, regulation of translation, transcription
33	Nucleophosmin 1 isoform 3	IPI00658013	Up	34	308	28,383	4.56	1.10E-26	NF-kappaB binding, RNA binding, Tat protein binding, histone binding, protein heterodimerization activity, protein homodimerization activity, transcription coactivator activity, unfolded protein binding,	Anti-apoptosis, cell aging, centroso me cycle, interspecies interaction between organisms, intracellular protein transport, negative regulation of cell proliferation, negative regulation of centrosome duplication, nucleocytoplasmic transport, nucleosome assembly, positive regulation of NF-kappaB transcription factor activity, protein localization, response to stress, ribosome assembly, signal transduction.

34	Keratin, type II cytoskeletal 1 (KKRT1)	IPI00220327	Up	25	315	65,847	8.16	2.10E-27	Protein binding, receptor activity, structural constituent of cytoskeleton, sugar binding	Complement activation, lectin pathway, epidermis development, fibrinolysis, regulation of angiogenesis, response to oxidative stress
37	Isoform 1 of RNA-binding protein 8A (RBM8A)	IPI00001757	Up	33	111	19,877	5.5	5.30E-07	mRNA binding, nucleotide binding, protein binding	RNA splicing, biological process, mRNA catabolic process, nonsense-mediated decay, mRNA processing, mRNA transport, transport
38	DnaJ homolog subfamily C member 9(DNAJC9)	IPI00154975	Up	57	336	29,891	5.58	1.70E-29	Heat shock protein binding	Unknown

was TGCAGTCCTCGCTCACTGGGCACG. All the RNA determinations were assayed in duplicate and repeated three times.

3. Results

3.1. Changes in the A549 cell nucleus proteome profile upon infection

The fractions of A549 cell nuclear proteins from the controls and samples at 36 h after infection were loaded onto pH 4–7 IPG strips, and 2-DE was performed. Three gel images for each sample were analyzed using the Image Master 2D Platinum software. The representative expression patterns are shown in Fig. 1A. Based on the normalized volume of each spot, we analyzed the differential expression of proteins between the control and infected groups. Forty spots were found to be differentially expressed in the infected group at 36 h after inoculation. Eighteen spots showed increased expression and 22 spots showed decreased expression in the 36 h group as compared to spots from the control group. Fig. 1B shows a high-power 2-DE image of seven spots. The purity of subcellular fractions was confirmed by observing the nucleus by contrast-phase microscopy, combined with western blot analysis for the actin and cytochrome *c* proteins in the subcellular fractions (Fig. 1 C and D). As shown by the morphology and apoptosis data, maximal epithelial cell infection of the influenza virus was observed at 36 h, which slightly reduced at 48 h (Fig. 1E and F). In a separate experiment, viral M1 protein expression in the host cells increased after infection and did not significantly changed from 36 to 48 h (unpublished data). In addition, the influenza virus (HIN1)-A549 cell infection was confirmed by detecting NP expression in the nuclear and cytosolic fractions at various time points post infection (Fig. 1G). Based on these data, the 36 h time point was chosen for proteomic analysis.

3.2. Identification of differentially expressed nuclear proteins

To identify differentially expressed nuclear proteins, protein spots described in 3.1 were prepared for MALDI-TOF MS analysis. The peptide mass peaks were compared with those in the National Council for Biotechnology Information (NCBI) database. Thirty protein spots were successfully identified from the H1N1 infected group and are listed in Table 1. A typical mass spectrum of the in-gel tryptic digestion generated from spot 27 is shown in Fig. 2, and the identification of this mass spectrum was stress-70 protein, a mitochondrial precursor. Nineteen peptides matched the theoretical masses with 37% coverage of amino acid sequence.

3.3. Changes in the A549 mitochondrial and cytosolic proteome profile after infection

Fractions of the A549 mitochondrial and cytosolic proteins from the control and infected samples were also performed using 2-DE in the pH 4–7 range as described above. Supplemental Fig. 1 shows representative 2-DE images of mitochondrial fractions isolated from the infected A549 cells and control. Twenty protein spots were found to be differentially expressed at 36 h post infection. A total of 13 protein spots were successfully identified by MALDI-TOF MS, and the results are summarized in Table 2. Most of these proteins are involved in mitochondrial energy metabolism and protein binding. Supplemental Fig. 2 shows 2-DE images of cytosolic fractions isolated from control and influenza H1N1-infected A549 cells. Analysis of the gel images revealed 52 protein spots differentially expressed at 36 h after infection. A total of 37 proteins were identified by MALDI-TOF MS at this 36 h time point, and the results are summarized in Table 3.

A

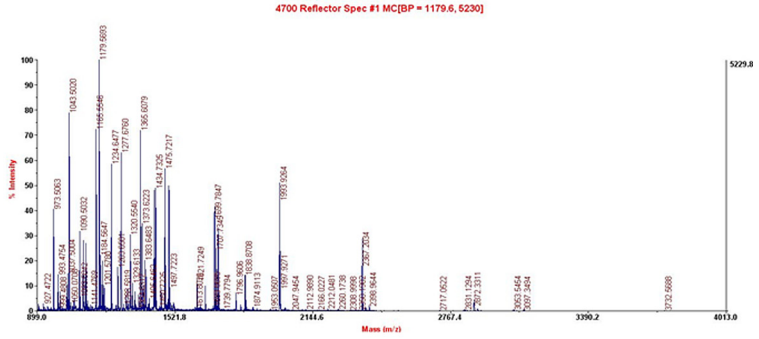

B

```
  1 MISASRAAAA RLVGAAASRG PTAARHQDSW NGLSHEAFRL VSRRDYASEA
 51 IKGAVVGIDL GTTNSCVAVM EGKQAKVLEN AEGARTTPSV VAFTADGERL
101 VGMPAKRQAV TNPNNTFYAT KRLIGRRYDD PEVQKDIKNV PFKIVRASNG
151 DAWVEAHGKL YSPSQIGAFV LMKMKETAEN YLGHTAKNAV ITVPAYFNDS
201 QRQATKDAGQ ISGLNVLRVI NEPTAAALAY GLDKSEDKVI AVYDLGGGTF
251 DISILEIQKG VFEVKSTNGD TFLGGEDFDQ ALLRHIVKEF KRETGVDLTK
301 DNMALQRVRE AAEKAKCELS SSVQTDINLP YLTMDSSGPK HLNMKLTRAQ
351 FEGIVTDLIR RTIAPCQKAM QDAEVSKSDI GEVILVGGMT RMPKVQQTVQ
401 DLFGRAPSKA VNPDEAVAIG AAIQGGVLAG DVTDVLLLDV TPLSLGIETL
451 GGVFTKLINR NTTIPTKKSQ VFSTAADGQT QVEIKVCQGE REMAGDNKLL
501 GQFTLIGIPP APRGVPQIEV TFDIDANGIV HVSAKDKGTG REQQIVIQSS
551 GGLSKDDIEN MVKNAEKYAE EDRRKKERVE AVNMAEGIIH DTETKMEEFK
601 DQLPADECNK LKEEISKMRE LLARKDSETG ENIRQAASSL QQASLKLFEM
651 AYKKMASERE GSGSSGTGEQ KEDQKEEKQ
```

C

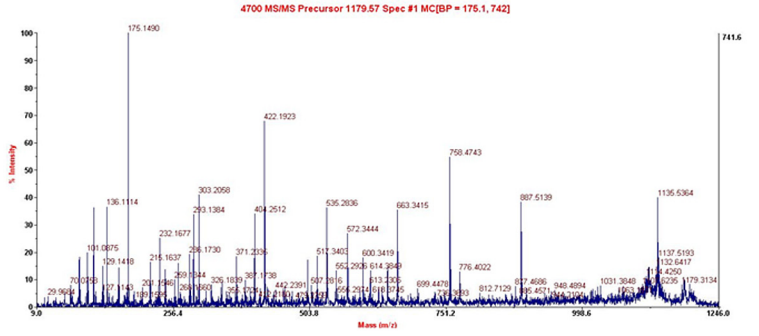

D

MONOISOTOPIC mass of neutral peptide Mr(calc): 1693.8423
Ions Score: 105 Expect: 6.9e-009
Matches (Bold Red): 29/256 fragment ions using 24 most intense peaks

#	Immon.	a	a*	a^0	b	b*	b^0	Seq.	v	w	w*	y	y*	y^0	#
1	87.0553	87.0553	70.0287		115.0502	98.0237		N							15
2	44.0495	158.0924	141.0659		**186.0873**	**169.0608**		A	1564.7754			**1580.8067**	1563.7802	1562.7961	14
3	**72.0808**	257.1608	240.1343		**285.1557**	268.1292		V	1465.7070	1478.7274		1509.7696	1492.7431	1491.7590	13
4	86.0964	370.2449	353.2183		**398.2398**	381.2132		I	1352.6229	1365.6433	1379.6590	**1410.7012**	1393.6746	1392.6906	12
5	74.0600	471.2926	454.2660	453.2820	499.2875	482.2609	**481.2769**	T	1251.5753	1264.5957	1266.5749	**1297.6171**	1280.5906	1279.6066	11
6	**72.0808**	570.3610	553.3344	552.3504	598.3559	581.3293	**580.3453**	V	1152.5069	1165.5273		**1196.5695**	**1179.5429**	1178.5589	10
7	70.0651	667.4137	650.3872	649.4032	695.4086	678.3821	677.3981	P	**1055.4541**	1054.4588		**1097.5010**	**1080.4745**	1079.4905	9
8	44.0495	738.4508	721.4243	720.4403	**766.4457**	749.4192	748.4352	A	984.4170			1000.4483	983.4217	982.4377	8
9	136.0757	901.5142	884.4876	883.5036	**929.5091**	912.4825	911.4985	Y	821.3537			**929.4112**	912.3846	911.4006	7
10	120.0808	1048.5826	1031.5560	1030.5720	1076.5775	1059.5509	1058.5669	F	674.2852			**766.3478**	749.3213	748.3373	6
11	87.0553	1162.6255	1145.5990	1144.6149	1190.6204	1173.5939	1172.6099	N	560.2423	559.2471		619.2794	**602.2529**	601.2689	5
12	88.0393	1277.6524	1260.6259	1259.6419	1305.6474	1288.6208	1287.6368	D	445.2154	444.2201		**505.2365**	488.2100	487.2259	4
13	60.0444	1364.6845	1347.6579	1346.6739	1392.6794	1375.6528	1374.6688	S	358.1833	357.1881		**390.2096**	373.1830	372.1990	3
14	101.0709	1492.7431	1475.7165	1474.7325	1520.7380	1503.7114	1502.7274	Q	230.1248	229.1295		**303.1775**	286.1510		2
15	129.1135							R	74.0237	73.0284		**175.1190**	158.0924		1

Seq	ya	yb	Seq	ya	yb	Seq	ya	yb
AV	143.1179	171.1128	AVI	256.2019	284.1969	AVIT	357.2496	385.2445
AVITV	456.3180	484.3129	AVITVP	553.3708	581.3657	AVITVPA	624.4079	652.4028
VI	185.1648	213.1597	VIT	286.2125	314.2074	VITV	385.2809	413.2758
VITVP	482.3337	510.3286	VITVPA	553.3708	581.3657	IT	187.1441	215.1390
ITV	286.2125	314.2074	ITVP	383.2653	411.2602	ITVPA	454.3024	482.2973
ITVPAY	617.3657	645.3606	TV	173.1285	201.1234	TVP	270.1812	298.1761
TVPA	341.2183	369.2132	TVPAY	504.2817	532.2766	TVPAYF	651.3501	679.3450
VP	**169.1335**	197.1284	VPA	240.1706	268.1656	VPAY	403.2340	431.2289
VPAYF	550.3024	578.2973	VPAYFN	664.3453	692.3402	PA	141.1022	**169.0971**
PAY	304.1656	332.1605	PAYF	451.2340	479.2289	PAYFN	565.2769	593.2718
PAYFND	680.3038	708.2988	AY	207.1128	235.1077	AYF	354.1812	382.1761
AYFN	468.2241	496.2191	AYFND	583.2511	611.2460	AYFNDS	670.2831	698.2780
YF	283.1441	311.1390	YFN	397.1870	425.1819	YFND	512.2140	540.2089
YFNDS	599.2460	627.2409	FN	234.1237	262.1186	FND	349.1506	377.1456
FNDS	436.1827	464.1776	FNDSQ	564.2413	592.2362	ND	202.0822	230.0771
NDS	289.1143	317.1092	NDSQ	417.1728	445.1678	DS	**175.0713**	203.0662
DSQ	**303.1299**	331.1248	SQ	188.1030	216.0979			

Fig. 2. MS and identification of spot 27. (A) Mass spectrum of spot 27 obtained by MALDI-TOF-MS. (B) Identification of spot 27 as stress-70 protein, a mitochondrial precursor (GRP 75) with 37% amino acid sequence coverage by matched peptides (red) by using Mascot software. (C) Mass spectrum of spot 27 obtained by MALDI-TOF-MS/MS. (D) MS/MS fragmentation of NAVITVPAYFNDSQR and identification of spot 27 as GRP 75. (For interpretation of the references to colour in this figure legend, the reader is referred to the web version of this article.)

Table 2
Identified proteins that changed significantly in A549 cell mitochondria after infection.

Spot no.	Protein	Accession no.	Up/down regulated (>2-fold)	Sequence coverage (%)	Score	Mass	*pI*	*P* value	Function	Process
1	12 kDa Protein, macrophage migration inhibitory factor (MIF)	IPI00790382	Up	20	66	11,947	9.3	0.016	Cytokine activity, isomerase activity, phenylpyruvate tautomerase activity, protein binding	Cell proliferation, cell surface receptor linked signal transduction, inflammatory response, negative regulation of apoptosis, prostaglandin biosynthetic process, regulation of macrophage activation
2	Actin, cytoplasmic 1	IPI00021439	Down	5	92	41,710	5.29	4.00E-05	Protein binding, structural constituent of cytoskeleton, ATP binding, nucleotide binding	Cell motility, sensory perception of sound
3	Interferon-induced 17 kDa protein precursor (ISG15)	IPI00375631	Up	23	194	17,745	7.03	2.70E-15	Protein binding, protein tag	Modification-dependent protein catabolic process, cell–cell signaling, ISG15-protein conjugation, ubiquitin cycle, response to virus
4	Peroxiredoxin-1	IPI00000874	Down	33	187	22,096	8.27	1.30E-14	Oxidoreductase activity, peroxiredoxin activity, protein binding	Cell proliferation, cell redox homeostasis, hydrogen peroxide catabolic process, oxidation reduction, skeletal system development
7	Phosphatidylethanolamine-binding protein 1	IPI00219446	Up	28	124	20,913	7.42	2.70E-08	ATP binding, lipid binding, nucleotide binding, phosphatidylethanolamine binding, protein binding, serine-type endopeptidase inhibitor activity	Unknown
8	BLVRB biliverdin reductase B (flavin reductase (NADPH))	IPI00783862	Up	34	193	21,974	7.31	3.30E-15	Biliverdin reductase activity, binding, coenzyme binding, flavin reductase activity, oxidoreductase activity	Cellular metabolic process
9	93 kDa Protein, TTN titin isoform N2-A	IPI00749039	Down	13	74	92,723	5.13	0.003	ATP binding, Rho guanyl-nucleotide exchange factor activity, alpha-actinin binding, calmodulin binding, cysteine-type endopeptidase activity, identical protein binding, myosin binding, nucleotide binding, protein serine/threonine kinase activity, structural constituent of muscle, transferase activity	Mitosis, myofibril assembly, protein amino acid autophosphorylation, proteolysis, regulation of Rho protein signal transduction, striated muscle contraction
10	Stress-70 protein, mitochondrial precursor (HSPA9)	IPI00007765	Down	23	160	73,635	5.87	6.70E-12	ATP binding, nucleotide binding, unfolded protein binding	Anti-apoptosis, protein export from nucleus, protein folding
13	ATP synthase subunit beta, mitochondrial precursor (ATP5B)	IPI00303476	Down	48	583	56,525	5.26	3.30E-54	ATP binding, contributes to ATPase activity, MHC class I protein binding, eukaryotic cell surface binding, hydrogen ion transporting ATP synthase activity, rotational mechanism, hydrogen-exporting ATPase activity, phosphorylative mechanism, hydrolase activity, hydrolase activity, acting on acid anhydrides, catalyzing transmembrane movement of substances, protein binding, nucleotide binding, proton-transporting ATPase activity, rotational mechanism, transporter activity	ATP synthesis coupled proton transport, angiogenesis, generation of precursor metabolites and energy, ion transport, lipid metabolic process, negative regulation of cell adhesion involved in substrate-bound cell migration, proton transport, regulation of intracellular pH
14	Heat-shock protein beta-1 (HSPB1)	IPI00025512	Down	37	290	22,768	5.98	6.70E-25	Identical protein binding	Anti-apoptosis, cell motility, regulation of translational initiation, response to unfolded protein
15	Isoform 1 of heat shock cognate 71 kDa protein (HSPA8)	IPI00003865	Down	23	160	70,854	5.37	6.70E-12	ATP binding, ATPase activity, coupled, nucleotide binding, protein binding	Protein folding, response to stress, response to unfolded protein
17	PREDICTED: similar to zinc finger protein 616	IPI00083235	Up	26	67	117,512	9.51	1.40E-02	Unknown	Unknown
19	B2M protein (B2M)	IPI00796379	Up	35	121	13,688	6.06	5.30E-08	MHC class I receptor activity	Antigen presentation, endogenous antigen, antigen processing, endogenous antigen via MHC class I, immune response

Table 3
Identified proteins that changed significantly in the A549 cell cytosol after infection.

Spot no.	Protein	Accession no.	Up/down regulated (>2-fold)	Sequence coverage (%)	Score	Mass	*pI*	P value	Function	Process
1	Heat-shock protein beta-1	IPI00025512	Up	45	350	22,768	5.98	6.70E-31	Identical protein binding,	Anti-apoptosis, cell motion, regulation of translational initiation, response to heat, response to unfolded protein
2	Annexin A1 (ANXA1)	IPI00218918	Up	46	658	38,559	6.64	1.10E-61	Calcium ion binding, calcium-dependent phospholipid binding, phospholipase A2 inhibitor activity, phospholipase inhibitor activity, protein binding, bridging, receptor binding, structural molecule activity	Anti-apoptosis, arachidonic acid secretion, cell cycle, cell motility, cell surface receptor linked signal transduction, inflammatory response, keratinocyte differentiation, lipid metabolic process, peptide cross-linking, regulation of cell proliferation
3	Isoform 3 of tropomyosin 1 alpha chain (TPM1)	IPI00216135	Up	50	354	32,856	4.72	2.70E-31	Actin binding, structural constituent of cytoskeleton, structural constituent of muscle	Cell motility, regulation of heart contraction, regulation of muscle contraction
7	ENO1, isoform MBP-1 of alpha-enolase	IPI00759806	Up	42	211	36,905	5.93	5.30E-17	Lyase activity, magnesium ion binding, phosphopyruvate hydratase activity, plasminogen activator activity, protein binding, transcription corepressor activity, transcription factor activity	Glycolysis, negative regulation of cell growth, negative regulation of transcription from RNA polymerase II promoter, transcription
8	Enolase 1	IPI00465248	Up	32	354	47,139	7.01	2.70E-31	Lyase activity, magnesium ion binding, phosphopyruvate hydratase activity, plasminogen activator activity, protein binding, serine-type endopeptidase activity, transcription corepressor activity, transcription factor activity	Glycolysis, negative regulation of cell growth, negative regulation of transcription from RNA polymerase II promoter, transcription
9	Keratin, type II cytoskeletal 1 (KRT1)	IPI00220327	Up	28	566	65,847	8.16	1.70E-52	Protein binding, receptor activity, structural constituent of cytoskeleton, sugar binding	Complement activation, lectin pathway, epidermis development, fibrinolysis, regulation of angiogenesis, response to oxidative stress
10	DMD, dystrophin Dp427l isoform	IPI00375141	Up	8	66	412144	5.6	0.019	Actin binding, calcium ion binding, protein binding, structural constituent of cytoskeleton, structural constituent of muscle, zinc ion binding	Cytoskeletal anchoring, muscle contraction, muscle development, peptide biosynthetic process
12	Uncharacterized protein PDIA3, 55 kDa protein (PDIA3)	IPI00657680	Up	18	123	54,929	6.42	3.30E-08	Cysteine-type endopeptidase activity, isomerase activity, phospholipase C activity, protein binding, protein disulfide isomerase activity	Cell redox homeostasis, positive regulation of apoptosis, protein import into nucleus, protein retention in ER, signal transduction
13	PKM2, isoform M2 of pyruvate kinase isozymes M1/M2, pyruvate kinase 3 isoform 1	IPI00479186	Up	34	361	57,900	7.96	5.30E-32	Magnesium ion binding, potassium ion binding, protein binding, pyruvate kinase activity, transferase activity	Glycolysis
14	GLO1 lactoylglutathione lyase	IPI00220766	Down	19	68	20,575	5.25	0.012	Lactoylglutathione lyase activity, lyase activity, metal ion binding, zinc ion binding	Anti-apoptosis, carbohydrate metabolic process
15	SET SET translocation (myeloid leukemia-associated)	IPI00646059	Down	17	70	31,114	4.09	0.007	Histone binding, protein phosphatase inhibitor activity, protein phosphatase type 2A regulator activity	DNA replication, negative regulation of histone acetylation, nucleocytoplasmic transport, nucleosome assembly, nucleosome disassembly
16	Ubiquitin carboxyl-terminal hydrolase isozyme L1 (UCHL1)	IPI00018352	Down	31	203	24,808	5.33	3.30E-16	Cysteine-type endopeptidase activity, ligase activity, omega peptidase activity, protein binding, ubiquitin binding, ubiquitin thiolesterase activity	Protein deubiquitination, ubiquitin-dependent protein catabolic process
18	ARG1 isoform 3 of arginase-1	IPI00038356	Down	21	67	25,469	8.35	0.014	Arginase activity, hydrolase activity, manganese ion binding, metal ion binding	Arginine catabolic process, urea cycle
19	Peroxiredoxin-6 (PRDX6)	IPI00220301	Down	21	132	24,888	6.02	4.20E-09	Hydrolase activity, oxidoreductase activity, peroxiredoxin activity, phospholipase A2 activity	Lipid catabolic process, phospholipid catabolic process, response to oxidative stress
21	Annexin A1 (ANXA1)	IPI00218918	Down	12	65	38,559	6.64	0.021	Calcium ion binding, calcium-dependent phospholipid binding, phospholipase A2 inhibitor activity, phospholipase inhibitor activity, protein binding, bridging, receptor binding, structural molecule activity	Anti-apoptosis, arachidonic acid secretion, cell cycle, cell motility, cell surface receptor linked signal transduction, inflammatory response, keratinocyte differentiation, lipid metabolic process, peptide cross-linking, regulation of cell proliferation

22	Isoform 1 of arginase-1 (ARG1)	IPI00291560	Down	19	64	34,713	6.72	0.029	Arginase activity, hydrolase activity, manganese ion binding, metal ion binding	Arginine catabolic process, urea cycle
23	ACTB actin, cytoplasmic 1 (ACTB)	IPI00021439	Down	26	99	41,710	5.29	8.20E-06	ATP binding, nucleotide binding, protein binding, structural constituent of cytoskeleton	Cell motility, sensory perception of sound
26	Enolase 1	IPI00465248	Down	26	149	47,139	7.01	8.40E-11	Lyase activity, magnesium ion binding, phosphopyruvate hydratase activity, plasminogen activator activity, protein binding, serine-type endopeptidase activity, transcription corepressor activity, transcription factor activity	Glycolysis, negative regulation of cell growth, negative regulation of transcription from RNA polymerase II promoter, transcription
27	Keratin, type I cytoskeletal 10 (KRT10)	IPI00009865	Down	25	103	59,483	5.13	3.30E-06	Protein binding, structural constituent of epidermis	Epidermis development
29	Isoform 2 of G protein-regulated inducer of neurite outgrowth 1 (GPRIN1)	IPI00744232	Down	17	69	80,870	8.74	0.0084	Phosphoprotein binding	Neurite development
30	Heat-shock protein beta-1	IPI00025512	Down	56	460	22,768	5.98	6.7e-042	Identical protein binding	Anti-apoptosis, cell motility, regulation of translational initiation, response to unfolded protein
31	26 kDa Protein	IPI00790768	Down	62	317	26,068	5	1.30E-27	Unknown	Unknown
32	Proteasome subunit alpha type-5 (PSMA5)	IPI00291922	Down	59	428	26,394	4.74	1.10E-38	Protein binding, threonine endopeptidase activity	Ubiquitin-dependent protein catabolic process
33	Heat shock protein HSP 90-alpha 2	IPI00382470	Down	16	254	98,099	5.07	2.70E-21	unfolded protein binding, molecular_function	protein folding, biological_process
34	Hematological and neurological expressed 1 isoform 1	IPI00007764	Down	37	118	16,005	5.47	1.10E-07	Unknown	Unknown
36	Programmed cell death protein 5 (PDCD5)	IPI00023640	Up	50	196	14,145	5.78	1.70E-15	DNA binding	Apoptosis, induction of apoptosis
38	Annexin A5 (ANXA5)	IPI00329801	Down	56	531	35,783	4.94	5.30E-49	Calcium ion binding, calcium-dependent phospholipid binding, phospholipase inhibitor activity	Blood coagulation, negative regulation of coagulation
39	Actin, cytoplasmic 1	IPI00021439	Up	49	473	41,710	5.29	3.30E-43	ATP binding, nucleotide binding, protein binding, structural constituent of cytoskeleton	Cell motility, sensory perception of sound
40	Elongation factor 2 (EEF2)	IPI00186290	Up	21	366	95,146	6.42	1.70E-32	GTP binding, Translation elongation factor activity	Protein biosynthesis
41	Actin, cytoplasmic 1	IPI00021439	Up	37	385	41,710	5.29	2.10E-34	ATP binding, nucleotide binding, protein binding, structural constituent of cytoskeleton	Cell motility, sensory perception of sound
42	Actin, cytoplasmic 1	IPI00021439	Up	25	323	41,710	5.29	3.3e-028	ATP binding, nucleotide binding, protein binding, structural constituent of cytoskeleton	Cell motility, sensory perception of sound
43	Actin, cytoplasmic 1	IPI00021439	Up	18	319	41,710	5.29	8.4e-028	ATP binding, nucleotide binding, protein binding, structural constituent of cytoskeleton	Cell motility, sensory perception of sound
44	Actin, cytoplasmic 1	IPI00021439	Up	25	425	41,710	5.29	2.1e-038	ATP binding, nucleotide binding, protein binding, structural constituent of cytoskeleton	Cell motility, sensory perception of sound
45	21 kDa Protein (TAGLN2)	IPI00644531	Up	50	234	21,073	7.63	2.70E-19	Protein binding	Muscle development
46	Glyceraldehyde 3-phosphate dehydrogenase (GAPDH)	IPI00789134	Up	20	231	27,853	6.45	5.30E-19	NAD binding, binding, catalytic activity, glyceraldehyde-3-phosphate dehydrogenase (phosphorylating) activity, oxidoreductase activity, protein binding	Glucose metabolic process, glycolysis, metabolic process
47	26 kDa Protein	IPI00790768	Up	52	313	26,068	5	3.30E-27	Unknown	Unknown
48	Actin, cytoplasmic 1	IPI00021439	Up	51	419	41,710	5.29	8.4e-038	ATP binding, nucleotide binding, protein binding, structural constituent of cytoskeleton	Cell motility, sensory perception of sound

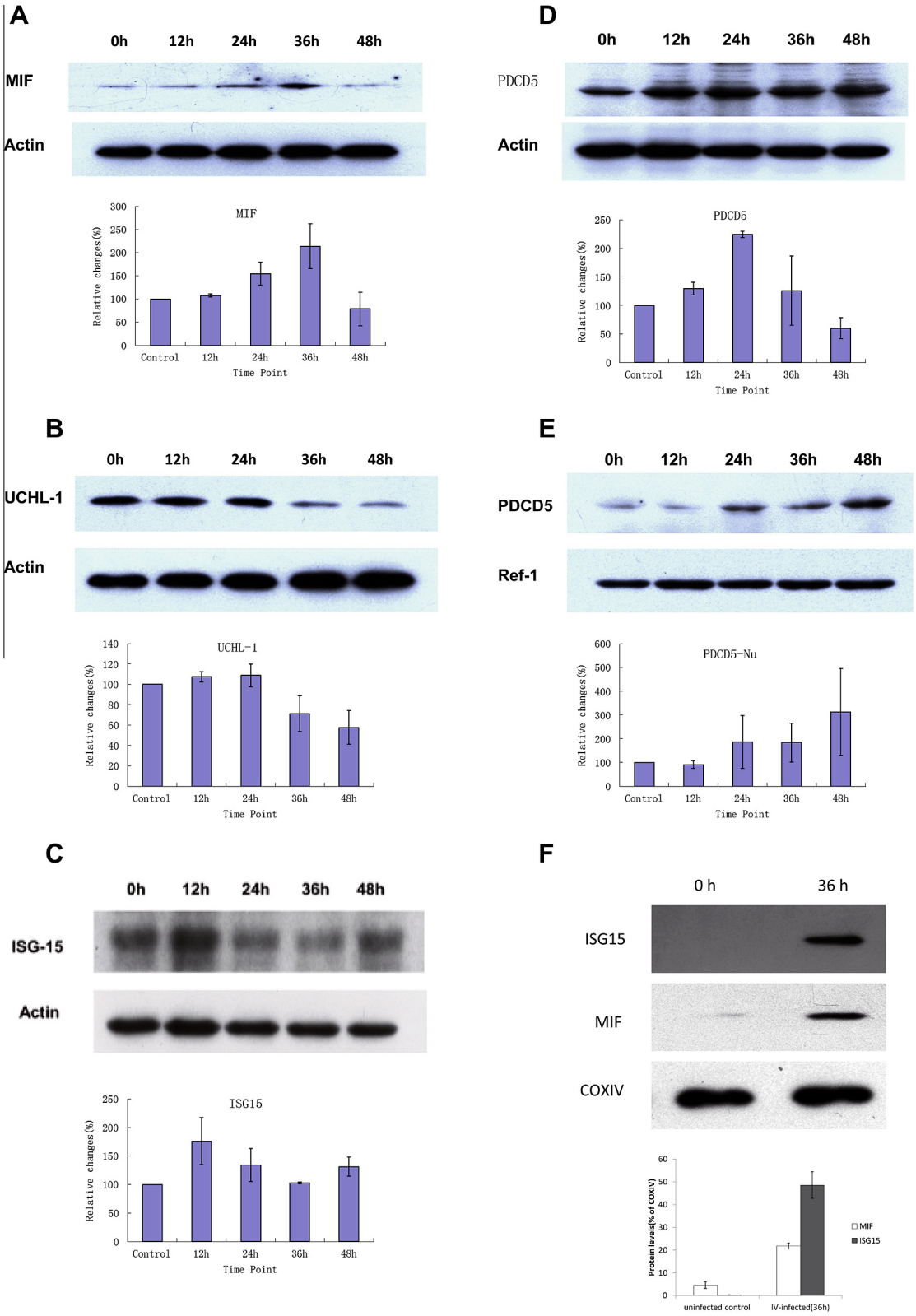

Fig. 3. Western blotting analysis of MIF, ISG15, UCHL1, and PDCD5 from cytosolic gradients. Mitochondrial and cytosolic proteins from control and IV infected A549 cells (after 36 h of inoculation) were separated and transferred to PVDF membranes as described in Section 2. The bands were probed using anti-MIF (A), anti-UCHL1 (B), anti-ISG15 antibody (C), and anti-PDCD5 antibody in the cytoplasm (D) and anti-PDCD5 antibody in the nucleus (E). The MIF and ISG15 protein levels in the mitochondria fraction at 36 h after influenza virus infection is shown in (F). Actin was used the reference protein for the cytoplasm protein and the Ref-1 was used as reference protein for the nuclear protein. Data shown are representative of three independent experiments.

A

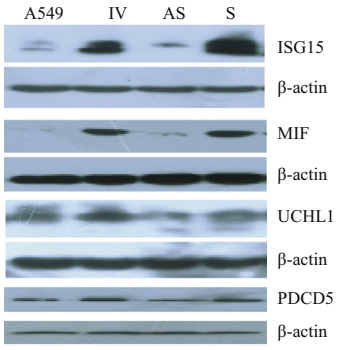

B

Gene name	Length (nt)	Sequence (5-3')	IC50±SD (μM)
ISG15	20	GCCAGCATCTTCACCGTCAG	0.533±0.048
MIF	20	GAGTTGTTCCAGCCCACATT	0.592±0.042
PDCD5	20	GCTTCCCTGTGCTTTGCTTC	0.288±0.062
UCHL1	20	CTTGTCCCTTCAGCTCTTCA	0.535±0.234

C

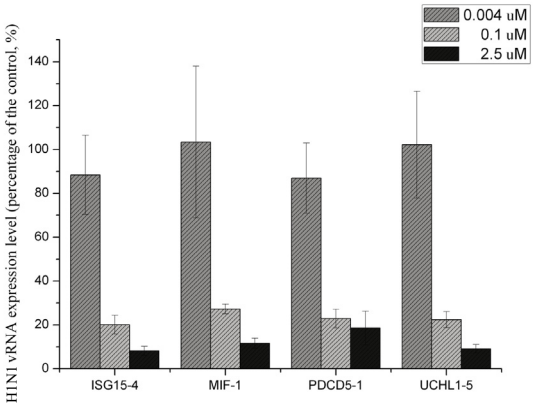

D

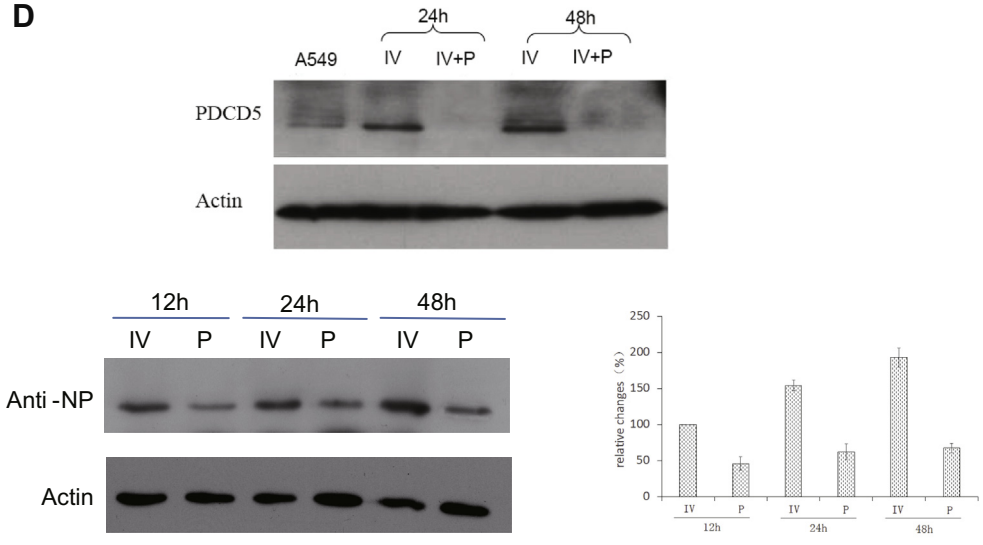

Fig. 4. Effects of ODNs on influenza virus vRNA in A549 cells. (A) ODNs that target PDCD5, ISG15, MIF, or UCHL1 inhibit protein expression of PDCD5, ISG15, MIF, or UCHL1, respectively, in influenza virus-infected A549 cells. AS, antisense ODN; S, sense sequence ODN. (B) The sequence of the ODNs, which target ISG15, MIF, PDCD5, and UCHL1, and the 50% inhibitory effect (IC50) of the ODNs on CPE (%) (cytopathic effect), $n = 4$. (C) Influenza virus-infected A549 cells were treated with ODNs, which target ISG15, MIF, PDCD5, and UCHL1. At 48 h post-transfection, vRNA copies in the infected cells were analyzed using qRT-PCR as described in Section 2. $n = 4$. (D) ODNs that target PDCD5 inhibit NP protein expression in influenza virus-infected A549 cells at various time points. P, PDCD5 antisense ODN. Actin was used as the reference protein for the cytoplasm protein. Data shown are representative of 3–4 independent experiments.

3.4. Validation of infection-induced proteins

To validate the protein expression patterns observed in this study, four proteins, that is, MIF, and ISG15 from the mitochondria and UCHL1 and PDCD5 from the cytosol, were selected for further study. Western blot analysis of subcellular fractions from control and infected A549 cells indicated that MIF, ISG15, and PDCD5 cytosolic protein levels initially increased post infection but were then normalized (Fig. 3A, C and D) Notably, UCHL1 did not exhibit any significant change at the beginning of the infection but was markedly reduced for 24 h in the cytosolic fraction of A549 cells after infection as compared to the control (Fig. 3B). In the nucleus, PDCD5 expression increased at 24 h after infection (Fig. 3E), while MIF and ISG15 mitochondrial levels increased at 36 h post infection (Fig. 3F). These results are in accordance with those obtained from the proteomics approach.

3.5. IV (H1N1) propagation in A549 cells was inhibited by silencing ISG15, MIF, PDCD5, or UCHL1 with ODNs

ODNs were designed to target ISG15, MIF, PDCD5, and UCHL1. ODN sequences were selected to target each gene at non-toxic doses and inhibit PDCD5, ISG15, MIF, or UCHL1 protein expression in influenza virus-infected A549 cells, respectively (Fig. 4A). As shown in Fig. 4B, the MIF, PDCD5, UCHL1, and ISG15 ODNs sequences significantly inhibit influenza virus (HIN1)-induced CPE; notably, the PDCD5 ODN exhibited the lowest IC_{50} value. The vRNA levels obtained from the IV-infected medium decreased in a dose dependent manner in the ISG15, MIF, PDCD5, and UCHL1 ODN-treated medium (Fig. 4C). Furthermore, inhibition of PDCD5 protein expression, which inhibits NP expression (Fig. 4D) in these influenza virus (HIN1)-infected A549 cells was observed, suggesting that PDCD5 may play a role in the processes of influenza virus (HIN1) vRNA synthesis.

4. Discussion

There are several advantages to applying proteomics research to subcellular fractions. Specifically, this will drastically reduce the complexity of a protein sample, reduce the possibility of protein spot overlapping, and potentially allow for the analysis of protein trafficking between organelles. In this study, three fractions extracted from the infected and normal A549 cells were analyzed by subcellular comparative proteomics to identify the proteins related to influenza A/jingfang/1/86 (H1N1) viral infection. This virus strain has previously been utilized to screen for anti-virus antisense ODNs both *in vitro* and *in vivo* and was particularly effective for ODN screening *in vivo* (Duan et al., 2008). A total of 112 protein spots were identified as differentially expressed proteins in the infected A549 cells as compared to the control. Most protein species alterations were associated with apoptosis and the heat shock protein family. Apoptotic proteins, which have previously been implicated in viral infections, such as ISG15, UCHL1, GRP75, MIF, and HSPA8 (Watanabe et al., 2006; Yuan and Krug, 2001), were significantly altered in the infected group as compared to the control. Importantly, inhibiting ISG15, MIF, PDCD5, and UCHL1 expression with ODNs prevented influenza virus propagation, thus suggesting that these proteins may be potential host therapeutic targets against influenza virus (HIN1) propagation in A549 cells. Since the 2D-MS method, which also detects host proteins, was utilized in this study, it is reasonable that influenza proteins were not detected. Virion proteomic analysis requires a different technical method, specifically, a highly purified preparation of virus which was not performed here (Shaw et al., 2008; Zheng et al., 2011).

ISG15 is an interferon-induced ubiquitin-like modifier (Osiak et al., 2005) that is conjugated to intracellular target proteins after IFN-α or IFN-β stimulation. ISG15 shows specific chemotactic activity toward neutrophils and activates neutrophils to induce the release of eosinophil chemotactic factors (Narasimhan et al., 1996). ISG15 is known to be involved in autocrine, paracrine, and endocrine mechanisms as seen in cell-to-cell signaling, likely due to its role in inducing IFN-γ secretion by monocytes and macrophages. The reports suggest that the host cell ISG15 protein might play a role in viral propagation. Our results indicate that A549 cells apoptosis induced by influenza virus (HIN1) was significantly reduced when ISG15 mRNA was inhibited with ODN. Interestingly, (Hsiang et al., 2009) also demonstrated that IFN-induced antiviral activity against influenza A virus in human cells is significantly alleviated by inhibiting ISG15 conjugation by using siRNAs directed against ISG15 conjugating enzymes. These data suggest that ISG15 is involved in the host cell immune response to influenza A virus infection. *UCHL1* is a member of the gene family whose products hydrolyze small C-terminal adducts of ubiquitin to generate the ubiquitin monomer. The ubiquitin-protein hydrolase is involved both in the processing of ubiquitin precursors and ubiquitinated proteins. Expression of UCHL1 is considered highly specific to neurons and to cells of the diffuse neuroendocrine system and their tumors (Doran et al., 1983). However, increasing evidence has shown that UCHL1 is involved in multiple diseases as well as the host cell's response to viral infections. Gao et al. reported that UCHL1 levels were markedly increased in Coxsackievirus B3-infected mice (Gao et al., 2008). Here, we provide evidence that UCHL1 may be involved in influenza viral infection. MIF plays an important role in the inflammatory response and plays a role in the regulation of macrophage activation (Miller et al., 2008). Since macrophages and other immune cells are activated after influenza virus infection, it is possible that MIF translocates in cells after influenza viral infections.

In summary, we have provided subcellular proteomic characterization of influenza virus (HIN1) infected human epithelial cells and identified some proteins that respond to infection. ISG15, MIF, PDCD5, and UCHL1 were differently expressed after influenza virus (HIN1) infection and inhibition of each of them mitigated influenza virus (HIN1) propagation in human cells, thus indicating that they could act as anti-IV host targets.

Funding

This work was supported by Grants from the State Key Program of National Natural Science of China (Grant No. 81230089), National Science Foundation for Young Scholars of China (Grant No. 30800978), and National Science Foundation of China (Grant No. 31270197).

Appendix A. Supplementary data

Supplementary data associated with this article can be found, in the online version, at http://dx.doi.org/10.1016/j.antiviral.2013.10.005.

References

Baas, T., Baskin, C.R., Diamond, D.L., Garcia-Sastre, A., Bielefeldt-Ohmann, H., Tumpey, T.M., Thomas, M.J., Carter, V.S., Teal, T.H., Van Hoeven, N., Proll, S., Jacobs, J.M., Caldwell, Z.R., Gritsenko, M.A., Hukkanen, R.R., Camp 2nd, D.G., Smith, R.D., Katze, M.G., 2006. Integrated molecular signature of disease: analysis of influenza virus-infected macaques through functional genomics and proteomics. J. Virol. 80, 10813–10828.

Bridges, C.B., Kuehnert, M.J., Hall, C.B., 2003. Transmission of influenza: implications for control in health care settings. Clin. Infect. Dis. 37, 1094–1101.

Chen, J., Deng, Y.M., 2009. Influenza virus antigenic variation, host antibody production and new approach to control epidemics. Virol. J. 6, 30.

Cohen, J., 2009. Swine flue outbreak. Flu researchers train sights on novel tricks of novel H1N1. Science 324, 870–871.
Doran, J.F., Jackson, P., Kynoch, P.A., Thompson, R.J., 1983. Isolation of PGP 9.5, a new human neurone-specific protein detected by high-resolution two-dimensional electrophoresis. J. Neurochem. 40, 1542–1547.
Duan, M., Zhou, Z., Lin, R.X., Yang, J., Xia, X.Z., Wang, S.Q., 2008. In vitro and in vivo protection against the highly pathogenic H5N1 influenza virus by an antisense phosphorothioate oligonucleotide. Antivir. Ther. 13, 109–114.
Ehrhardt, C., Ludwig, S., 2009. A new player in a deadly game: influenza viruses and the PI3K/Akt signalling pathway. Cell. Microbiol. 11, 863–871.
Ehrhardt, C., Wolff, T., Pleschka, S., Planz, O., Beermann, W., Bode, J.G., Schmolke, M., Ludwig, S., 2007. Influenza A virus NS1 protein activates the PI3K/Akt pathway to mediate antiapoptotic signaling responses. J. Virol. 81, 3058–3067.
Gao, G., Zhang, J., Si, X., Wong, J., Cheung, C., McManus, B., Luo, H., 2008. Proteasome inhibition attenuates coxsackievirus-induced myocardial damage in mice. Am. J. Physiol. Heart Circ. Physiol. 295, H401–408.
Gubareva, L.V., Webster, R.G., Hayden, F.G., 2002. Detection of influenza virus resistance to neuraminidase inhibitors by an enzyme inhibition assay. Antiviral Res. 53, 47–61.
He, Y., Xu, K., Keiner, B., Zhou, J., Czudai, V., Li, T., Chen, Z., Liu, J., Klenk, H.D., Shu, Y.L., Sun, B., 2010. Influenza A virus replication induces cell cycle arrest in G0/G1 phase. J. Virol. 84, 12832–12840.
Hsiang, T.Y., Zhao, C., Krug, R.M., 2009. Interferon-induced ISG15 conjugation inhibits influenza A virus gene expression and replication in human cells. J. Virol. 83, 5971–5977.
Kislinger, T., Cox, B., Kannan, A., Chung, C., Hu, P., Ignatchenko, A., Scott, M.S., Gramolini, A.O., Morris, Q., Hallett, M.T., Rossant, J., Hughes, T.R., Frey, B., Emili, A., 2006. Global survey of organ and organelle protein expression in mouse: combined proteomic and transcriptomic profiling. Cell 125, 173–186.
Li, C., Freedman, M., 2009. Seasonal influenza: an overview. J. Sch. Nurs. 25 (Suppl. 1), 4S–12S.
Lim, H., Eng, J., Yates 3rd, J.R., Tollaksen, S.L., Giometti, C.S., Holden, J.F., Adams, M.W., Reich, C.I., Olsen, G.J., Hays, L.G., 2003. Identification of 2D-gel proteins: a comparison of MALDI/TOF peptide mass mapping to mu LC-ESI tandem mass spectrometry. J. Am. Soc. Mass Spectrom. 14, 957–970.
Lin, R.X., Zhao, H.B., Li, C.R., Sun, Y.N., Qian, X.H., Wang, S.Q., 2009. Proteomic analysis of ionizing radiation-induced proteins at the subcellular level. J. Proteome Res. 8, 390–399.
Liu, N., Song, W., Wang, P., Lee, K., Chan, W., Chen, H., Cai, Z., 2008. Proteomics analysis of differential expression of cellular proteins in response to avian H9N2 virus infection in human cells. Proteomics 8, 1851–1858.
Mazur, I., Wurzer, W.J., Ehrhardt, C., Pleschka, S., Puthavathana, P., Silberzahn, T., Wolff, T., Planz, O., Ludwig, S., 2007. Acetylsalicylic acid (ASA) blocks influenza virus propagation via its NF-kappaB-inhibiting activity. Cell. Microbiol. 9, 1683–1694.
Miller, E.J., Li, J., Leng, L., McDonald, C., Atsumi, T., Bucala, R., Young, L.H., 2008. Macrophage migration inhibitory factor stimulates AMP-activated protein kinase in the ischaemic heart. Nature 451, 578–582.
Morens, D.M., Fauci, A.S., 2007. The 1918 influenza pandemic: insights for the 21st century. J. Infect. Dis. 195, 1018–1028.
Morrissey, B., Downard, K.M., 2006. A proteomics approach to survey the antigenicity of the influenza virus by mass spectrometry. Proteomics 6, 2034–2041.
Narasimhan, J., Potter, J.L., Haas, A.L., 1996. Conjugation of the 15-kDa interferon-induced ubiquitin homolog is distinct from that of ubiquitin. J. Biol. Chem. 271, 324–330.
Ohman, T., Rintahaka, J., Kalkkinen, N., Matikainen, S., Nyman, T.A., 2009. Actin and RIG-I/MAVS signaling components translocate to mitochondria upon influenza A virus infection of human primary macrophages. J. Immunol. 182, 5682–5692.
Osiak, A., Utermohlen, O., Niendorf, S., Horak, I., Knobeloch, K.P., 2005. ISG15, an interferon-stimulated ubiquitin-like protein, is not essential for STAT1 signaling and responses against vesicular stomatitis and lymphocytic choriomeningitis virus. Mol. Cell. Biol. 25, 6338–6345.
Shaw, M.L., Stone, K.L., Colangelo, C.M., Gulcicek, E.E., Palese, P., 2008. Cellular proteins in influenza virus particles. PLoS Pathog. 4, e1000085.
Shortridge, K.F., Gao, P., Guan, Y., Ito, T., Kawaoka, Y., Markwell, D., Takada, A., Webster, R.G., 2000. Interspecies transmission of influenza viruses: H5N1 virus and a Hong Kong SAR perspective. Vet. Microbiol. 74, 141–147.
Simonsen, L., 1999. The global impact of influenza on morbidity and mortality. Vaccine 17 (Suppl. 1), S3–S10.
Steiner, S., Gatlin, C.L., Lennon, J.J., McGrath, A.M., Aponte, A.M., Makusky, A.J., Rohrs, M.C., Anderson, N.L., 2000. Proteomics to display lovastatin-induced protein and pathway regulation in rat liver. Electrophoresis 21, 2129–2137.
Turpin, E., Luke, K., Jones, J., Tumpey, T., Konan, K., Schultz-Cherry, S., 2005. Influenza virus infection increases p53 activity: role of p53 in cell death and viral replication. J. Virol. 79, 8802–8811.
Watanabe, K., Fuse, T., Asano, I., Tsukahara, F., Maru, Y., Nagata, K., Kitazato, K., Kobayashi, N., 2006. Identification of Hsc70 as an influenza virus matrix protein (M1) binding factor involved in the virus life cycle. FEBS Lett. 580, 5785–5790.
Wurzer, W.J., Planz, O., Ehrhardt, C., Giner, M., Silberzahn, T., Pleschka, S., Ludwig, S., 2003. Caspase 3 activation is essential for efficient influenza virus propagation. EMBO J. 22, 2717–2728.
Yuan, W., Krug, R.M., 2001. Influenza B virus NS1 protein inhibits conjugation of the interferon (IFN)-induced ubiquitin-like ISG15 protein. EMBO J. 20, 362–371.
Zheng, J., Sugrue, R.J., Tang, K., 2011. Mass spectrometry based proteomic studies on viruses and hosts – a review. Anal. Chim. Acta 702, 149–159.